Trade-offs in ecosystem impacts from nanomaterial versus organic chemical ultraviolet filters in sunscreens

David Hanigan [a, *], Lisa Truong [c], Jared Schoepf [d], Takayuki Nosaka [d], Anjali Mulchandani [b], Robert L. Tanguay [c], Paul Westerhoff [b]

[a] Department of Civil and Environmental Engineering, University of Nevada, Reno, NV 89557-0258, United States
[b] School of Sustainable Engineering and the Built Environment, Nanosystems Engineering Research Center for Nanotechnology-Enabled Water Treatment, Arizona State University, Tempe, AZ 85287-3005, United States
[c] Environmental and Molecular Toxicology, Oregon State University, Corvallis, OR 97333, United States
[d] School for Engineering of Matter, Transport and Energy, Arizona State University, Tempe, AZ, 85287-5506, United States

ARTICLE INFO

ABSTRACT

Both nanoparticulate (nZnO and nTiO$_2$) and organic chemical ultraviolet (UV) filters are active ingredients in sunscreen and protect against skin cancer, but limited research exists on the environmental effects of sunscreen release into aquatic systems. To examine the trade-offs of incorporating nanoparticles (NPs) into sunscreens over the past two decades, we targeted endpoints sensitive to the potential risks of different UV filters: solar reactive oxygen production in water and disruption of zebrafish embryo development. First, we developed methodology to extract nanoparticles from sunscreens with organic solvents. Zebrafish embryos exposed to parts-per-million NPs used in sunscreens displayed limited toxicological effects; nZnO particles appeared to be slightly more toxic than nTiO$_2$ at the highest concentrations. In contrast, seven organic UV filters did not affect zebrafish embryogenesis at or near aqueous solubility. Second, to simulate potent photo-initiated reactions upon release into water, we examined methylene blue (MB) degradation under UV light. nTiO$_2$ from sunscreen caused 10 times faster MB loss than nZnO and approached the photocatalytic degradation rate of a commercial nTiO$_2$ photocatalysts (P25). Organic UV filters did not cause measurable MB degradation. Finally, we estimated that between 1 and 10 ppm of sunscreen NPs in surface waters could produce similar steady state hydroxyl radical concentrations as naturally occurring fluvic acids under sunlight irradiation. Incorporation of NPs into sunscreen may increase environmental concentrations of reactive oxygen, albeit to a limited extent, which can influence transformation of dissolved substances and potentially affect ecosystem processes.

© 2018 Elsevier Ltd. All rights reserved.

1. Introduction

Sunscreen use prevents skin cancer and has been increasing since its introduction to the commercial market by Eugene Schuéller and L'Oréal in 1936 (Cokkinides et al., 2006; Robinson et al., 1997). Organic chemical ultraviolet (UV) filters and micron-scale metal oxide particles were used exclusively as the active ingredients in sunscreen during the 20th century (Urbach, 2001). Nano-scale metal oxide particles such as titanium dioxide (nTiO$_2$) and zinc oxide (nZnO) absorb UV light but scatter relatively little visible light, and therefore the advent of nanotechnology provided materials that retained the UV filtering capability of micro-scale metal oxide particles and organic UV filters but are transparent to the human eye and do not degrade in the presence of UV light. Because of their low cost, desirable textural properties (non-greasy), and comparable UV filtering capability, metal oxide nanoparticles have become widely used active ingredients in commercial sunscreens during the past two decades. The increased incorporation into cosmetics (e.g., sunscreen, moisturizers, lip balm, etc.) of both organic and inorganic sunscreens has led to higher levels of human exposure and environmental loading (Balmer et al., 2005; Gondikas et al., 2014; Poiger et al., 2004; Venkatesan et al., 2018). Potential adverse environmental effects of these exposures must be balanced against benefits of human skin cancer prevention.

Two pathways of environmental release exist for UV filters: 1)

---

* Corresponding author.
  E-mail address: dhanigan@unr.edu (D. Hanigan).

recreational bathing resulting in acute exposure to aquatic species, and 2) wastewater discharges resulting in chronic exposure. The source of UV filters in wastewater is bathing (e.g., shower or bath water), or, for organic UV filters, partitioning through the dermis (up to 9% of the applied dose) (Hayden et al., 2005; Treffel and Gabard, 1996) and into the blood and eventual excretion in urine as the parent compound and metabolites (up to 2% of applied dose) (Hayden et al., 1997). Release through these pathways has resulted in detection of organic chemicals used as UV filters in treated wastewater and recreational waters at concentrations up to 65.4 and 0.2 nM, respectively (Balmer et al., 2005; Kupper et al., 2006; Poiger et al., 2004).

More than 20 organic UV filters have been approved by the European Union and US Food and Drug Administration (FDA) for use in sunscreen formulations and have undergone extensive testing regarding their mammalian toxicity (European Comission, 2009; Food and Drug Administration, 2016a). The estrogenic effects of organic UV filters both on animals (rainbow trout, Japanese medaka) and on human cells (Coronado et al., 2008; Schlumpf et al., 2001) has been studied, but no significant effects were observed until the applied dose was orders of magnitude greater (several μM) than would be expected in the environment (several nM) (Balmer et al., 2005; Poiger et al., 2004), or in cases of chronic exposure (Schlumpf et al., 2008). These studies suggest that the human and environmental risks of organic UV filter use are likely low, except in the case of waters heavily impacted by wastewater (chronic ecological exposure) or recreation (high dose acute exposure).

nTiO$_2$ and nZnO are also approved for use as UV filters by the FDA. Nano-scale formulations are not regulated separately from their micron-sized counterparts because the FDA does not consider these ingredients to be "new" from a regulatory perspective, rather a shift in size distribution of an already approved ingredient (Food and Drug Administration, 2016a). Additionally, nano-scale TiO$_2$ and nZnO have not shown the potential to pass the epidermis of healthy skins, and thus human effects are limited to the stratum corneum (no live cells and thus no potential for toxicity) (Gulson et al., 2010; Sadrieh et al., 2010). Based on available data, both inorganic and organic UV filters are relatively safe from a human endpoint perspective, and congruent with the FDA responsibility of, "Assuring cosmetics and dietary supplements are safe and properly labeled." (Food and Drug Administration, 2016b). But few studies directly investigated the aquatic environmental effects of sunscreen release. Nano-scale metal oxide UV filters are difficult to directly measure in natural waters, but several experimental and modeling studies have estimated that the maximum environmental concentrations would be in the low 10s of μg/L (David Holbrook et al., 2013; Gondikas et al., 2014; Johnson et al., 2011; Mueller and Nowack, 2008).

Nano-scale metal oxides, especially those commonly used as UV filters, nZnO and nTiO$_2$, are semiconductor photocatalysts and produce reactive oxygen species (ROS) in water, including superoxide and hydroxyl radicals, when exposed to UV light. Manufacturers are thought to have circumvented this potentially hazardous property by coating the particles with Al(OH)$_3$ and/or polydimethylsiloxane, but Auffan et al. (2010) suggests the coating may dissolve over time. However, efforts towards determining the environmental effects of nano-scale metal oxide sunscreen use has been almost solely focused on nTiO$_2$ UV filters that were purchased from chemical suppliers, rather than NPs extracted from sunscreens themselves, and may poorly represent NPs used in commercially available sunscreen formulations (Auffan et al., 2010; Foltête et al., 2011; Fouqueray et al., 2012; Labille et al., 2010). In general, few assessments exist with the capability to directly compare nano vs. chemical alternatives. Furthermore, legacy

fugacity-based fate and transport models are not directly applicable to NPs, but current efforts include developing models specific to NPs (Bouchard et al., 2017; Garner et al., 2017; Gottschalk et al., 2013; Liu and Cohen, 2014; Meesters et al., 2014; Praetorius et al., 2012; Westerhoff and Nowack, 2013). Therefore, researchers have called for targeted experiments and inclusion of new physiochemical property measurements that are specific to the hazardous properties of NPs, considering the intended use and potential release (Hjorth et al., 2016).

The goal of this study was to consider two endpoints after sunscreen release scenarios to assess the ecological trade-offs of replacing organic UV filters with nano-scale metal oxides. We studied seven organic UV filters (avobenzone, ecamsule, iscotrizinol, octocrylene, octyl methoxycinnamate, octyl salicylate, and oxybenzone) approved for use in either the European Union (iscotrizinol and ecamsule) or the European Union and the US. For inorganic metal oxides, a method was developed to extract the metal oxide particles from complex sunscreen matrices (five different sunscreens) and re-suspend them in water, and we compared their physical chemical properties to known ingredients commercially available for use in sunscreen products. We then used two endpoints to inform environmental implications in our study: 1) degradation of methylene blue (MB) to estimate ROS production during exposure to UV light and 2) zebrafish embryo development. The zebrafish embryo exposure experiment was used to determine acute developmental effects in an aquatic species that has a high potential for exposure. Finally, data was utilized to assess the potential trade-offs in risk of each class of UV filter.

2. Materials and methods

2.1. Sunscreens and reagents

Seven neat organic sunscreen active ingredients (i.e., oxybenzone, avobenzone, octyl salicylate, octyl methoxycinnamate, octocrylene, iscotrizinol, and ecamsule) were purchased from Sigma Aldrich (St. Louis, MO, USA) at ≥98% purity. Five sunscreens labeled as containing inorganic metal oxides were purchased from local supermarkets in Arizona (USA) in 2014. The purchased sunscreens were labeled as containing either zinc oxide or titanium dioxide, and a description of the labels is shown in Table 1. Aeroxide TiO$_2$ P25 and P90 powders were obtained from Evonik Industries (Essen, Germany). Two nano-scale zinc-based UV filters intended for commercial use in sunscreen products, one without a coating and one described by the vendor as having a hydrophobic coating (Z-Cote and Z-Cote HP1), were purchased directly from the vendor (TKBTrading, Oakland, CA USA) and used in control experiments as they were not incorporated into a complex sunscreen matrix. Reagent details can be found in the SI.

2.2. Sample preparation

Our extraction method was based on previous research that used organic solvents and centrifugation to separate the sunscreen matrix from the metal oxide particulate matter (Barker and Branch, 2008; Dunford et al., 1997; Lewicka et al., 2011; Rampaul et al., 2007). We explored several strategies to separate NPs from sunscreens, and our goal was to produce a method that was robust (insensitive to sunscreen brand), required as few extraction steps as possible to minimize changes in particle chemistry, and had the capacity for extraction to be visually confirmed during the process. Initial attempts to separate NP sunscreen matrix explored multiple solvents of varying polarity (dichloromethane [DCM] acetonitrile, methanol, and isopropanol). We believed that the matrix contained mostly non-polar compounds that would be soluble in non-polar

Table 1

Product identifiers and average particle sizes and standard deviation of 100—250 particles measured in the sunscreen extracts and in the as-purchased sunscreen. Particles were dispersed in ethanol and pipetted onto a copper TEM grid prior to analysis.

Identifier	Manufacturer	Product name	Sun protection factor	Labeled metal oxide active ingredients	Final size after extraction, 24 h settling, decantation (nm)	Centrifugation extract dispersed directly in ethanol (nm)	Centrifugation oil emulsion layer dispersed in ethanol (nm)
A	Coppertone	Kids tear free	50	14.5% ZnO	Length: 245 ± 149 Width: 67 ± 24	Length: 128 ± 51 Width: 51 ± 20	Length: 107 ± 57 Width: 41 ± 12
B	Dermatone	Moisturizing Lips 'n Face Protection Crème with Z-COTE	30	8.5% ZnO	Length: 712 ± 399 Width: 159 ± 83	Did not measure	Did not measure
C	Skinceuticals	Daily Sun Defense	20	5% ZnO	122 ± 58	136 ± 66	66 ± 29
D	Neutrogena	pure & free baby	60+	6.8% ZnO 8% TiO$_2$	Zn Length: 843 ± 397 Zn Width: 124 ± 58 Ti: 27 ± 10	Did not measure	Did not measure
E	Safeway	Kids Sunscreen Lotion	50	2.4% TiO$_2$	30 ± 10	40 ± 25	35 ± 22
Z-Cote	BASF	Z-Cote	NA	100% ZnO	105 ± 40	NA	NA
Z-Cote HP1	BASF	Z-Cote HP1	NA	100% ZnO	Length: 1678 ± 668 Width: 651 ± 232	NA	NA
P25	Evonik	P25	NA	100% TiO$_2$	21[a]	NA	NA
P90	Evonik	P90	NA	100% TiO$_2$	14[a]	NA	NA

[a] Manufacturer provided data of the raw material.

organic solvents. After attempting to disperse and separate particles via centrifugation from the matrix, we visually found that DCM provided the best separation (see results). The final extraction method follows. Approximately 5 g of sunscreen was placed in a 50 mL centrifuge tube with 20 mL DCM. The solution was vortexed, sonicated in a water bath for >5 min, and shaken vigorously until the solution appeared homogeneous. The solution was then centrifuged at 5000 RCF for 5 min. The two supernatant layers (oil emulsion and DCM layers) were decanted, leaving a solid white pellet. The white pellet was suspended in 20 mL of DCM, vortexed, sonicated again to re-disperse the pellet, and then centrifuged. We repeated this process a total of three times to remove organic constituents and oils while retaining the particulate matter, salts, and any surfactants contained in the sunscreen. We then used the same centrifugation and decantation method but substituted Milli-Q water as the solvent to remove salts and surfactants. This rinsing process was also repeated three times. The pellet was then washed one final time with 20 mL of DCM to remove any residual water, and we removed the residual solvent using a vacuum pump line attached to a one-holed stopper that fit the centrifuge tube. The vacuum was then released and the sample was capped and stored in room air. Additional sample preparation techniques including transmission electron microscopy (TEM) and quantification of metal in the extracted aqueous matrix are contained in the SI.

2.3. Particle characterization of extracted nanoparticles

Analysis by single particle inductively coupled plasma mass spectrometry (spICP-MS) was performed on non-digested samples using a Thermo Scientific X-Series II (Waltham, MA) in time resolved data acquisition mode with a dwell time of 10 ms following methodologies described elsewhere (Pace et al., 2011) and with details in the SI. In brief, extracted nanoparticles were placed in polypropylene sample tubes in either Milli-Q or pH 6 buffer, and the tubes were placed in a sonicating bath for 15 min. The samples were then immediately pumped into the instrument, and the spectra for ^{49}Ti and ^{66}Zn were recorded. We used three times the standard deviation of the spectra to delineate particle pulses from background dissolved metal.

TEM (Philips CM200, FEI, Hilsboro, OR, USA) with energy dispersive X-ray analysis (EDX) was used to measure particle size and elemental composition. Mean particle diameter was measured with ImageJ software. X-ray fluorescence (XRF, Niton XL3t GOLDD+, Thermo Fisher Scientific, Waltham, MA, USA), spICP-MS,

X-ray diffraction (XRD, X'Pert PRO MRD, PANalytical Inc. Netherlands), and dynamic light scattering (DLS) (ZetaPals, Brookhaven Instruments Corp, Holtsville, New York, USA) were also used to measure particle size, metal oxide composition, and crystalline structure. The refractive index for DLS measurements was set to 2.00 for samples containing nZnO and 2.63 for samples containing nTiO$_2$. XRD data was collected using a high-resolution X-ray diffractometer with Cu Ka radiation (45 kV, 40 mA) using a step scan mode. Diffractograms were collected in a 2θ range of 10—90° at a rate of 2°/min with a resolution of 0.025°.

2.4. UV photo-reactivity assay

We measured reaction kinetics between NP or organic UV filters and a probe compound (MB) in the presence of UV-B light (280—315 nm), similar to published approaches (Lee et al., 2011). The UV exposure apparatus was a 25W UVP Transilluminator (Upland, CA) producing 302 nm light. A 96-well plate reader was used to measure oxidation of MB at 650 nm. Nanoparticles extracted from sunscreens or organic UV filters were diluted into 96-well plates containing 10 mg/L MB and Milli-Q water or phosphate buffer. MB photodegradation or sorption to the plate wells was negligible when MB was placed in the wells in the absence of nanoparticles and exposed to UV light. MB sorption to the particles was also negligible during dark exposure experiments. Inorganic UV filters (nanoparticle extracts) were tested at multiple concentrations across multiple time points to obtain second order rate constants. Organic UV filters were tested at visible aqueous saturation. Plots of [MB] vs exposure duration were fit with an exponential function, and r^2 were typically greater than 0.9. If the exposure experiment resulted in a r^2 of less than 0.9, the experiment was repeated. This occurred only with P25 and P90, where the time resolution was too low in the initial experiment and the dye oxidation plateaued after less than three measurements.

2.5. Zebrafish assays

Tropical 5D wild-type adult zebrafish embryos were housed at Oregon State University Sinnhuber Aquatic Research Laboratory. Organic UV filters and nanoparticle extracts were shipped to Oregon State University and stored at 3 °C. Zebrafish assays were conducted within one month upon receipt of the samples. Embryos were dechorionated at 4 h post fertilization (hpf) and transferred into individual wells of a 96-well plate with 100 µL of prepared

nanoparticle solution. Nanoparticle solutions were diluted with their respective suspension media, either 0.1M pH 6 phosphate buffer or Milli-Q water to achieve the desired concentration in the well. Zebrafish were also exposed to the clean buffer solution of Milli-Q water. Embryos were statically exposed at 28 °C for 120 hpf to six concentrations (1/3 log change) of organic UV filters and nanoparticle extracts in replicates of 32 animals. Exposure plates were sealed to prevent evaporation and wrapped with aluminum foil to guard against potential photo-oxidation. At 24 and 120 hpf, 22 morphological endpoints were assessed according to Truong et al. (2011). A global control was computed per experiment day and used to determine statistical significance. Control animal development, combined with previous experience of the authors, demonstrated that the wells have enough head space such that the animals do not experience hypoxia during the experiment. Some morphological endpoints evaluated included mortality, developmental progression, and yolk sac edema. An additional two endpoints, "any effect except mortality" and "any effect," were calculated based on aggregate data from the 22 assayed endpoints. The criteria for statistical significance for these two endpoints is not automatically satisfied if a single of the other 20 endpoints is satisfied (i.e., statistically significant deviation from control samples for "any effect" and "any effect except mortality" does not necessarily mean statistically significant effects were observed in any of the other 22 individual endpoints).

The zebrafish acquisition and analysis program (ZAAP), a custom program designed to inventory, acquire, and manage zebrafish data, was used to collect developmental endpoints as either present or absent (i.e., binary responses were recorded). An internal quality assurance/quality control (QA/QC) plate consisting of 32 control animals and 32 animals exposed to 0.2 μM Ziram was also run each day to check for response consistency in the animals from different hatches. In the QA/QC plate, negative controls must exhibit less than 20% cumulative mortality and morbidity, and positive (Ziram) controls must display a notochord effect in at least 80% of the exposed animals. Statistical significance was computed as described in Truong et al. (2014) and Reif et al. (2016). Further details are provided in the SI.

3. Results and discussion

3.1. Extraction and characterization of UV filters in sunscreens

We based our initial methods to extract nanoparticles from sunscreens on prior research that used centrifugation methods with solvents of varying polarity (e.g., chloroform, acetone, isopropanol, methanol, and hexane) (Lewicka et al., 2011; Rampaul et al., 2007). DCM was determined to be the most practical solvent to achieve the key criterion of phase separation after homogenization with solvent followed by centrifugation. When the sunscreen was homogenized in methanol, it was difficult to visually distinguish a pellet because the white matrix emulsion components did not separate from the solvent phase (polymers, oils, etc.) and obscured the pellet. Isopropanol and acetonitrile had relatively transparent solvent phases, but the extracted material was visually more voluminous than a pellet of agglomerated metal oxide would be expected to appear after centrifugation. The extracted material likely included surfactants that are insoluble in isopropanol or acetonitrile. It may have been possible to later wash these surfactants out with water. However, DCM provided a density gradient separation, with much of the sunscreen emulsion constituents contained in a distinct white colored layer above a transparent DCM layer (Figure SI-1). DCM is also the most volatile of the solvents tested, and solvent removal was straightforward with the aid of a vacuum pump. Heating the extracted pellets (not used in

subsequent experiments) in air in a 550 °C furnace for 24 h resulted in less than 2.6% mass loss (organic matter) for all DCM extracted samples. Thus, the extracted pellets were nearly entirely inorganic material. While all solvents tested may have resulted in similar extracted products after multiple washings with organic solvent followed by water, we preferred to use DCM because we could visually observe the pellet, the pellet was composed of inorganic material based on thermal gravimetric measurements, and because DCM is highly volatile, allowing us to rapidly remove the solvent via a vacuum pump.

After separation from the sunscreen matrix, we characterized the extracted material. Initially, we used TEM to determine extracted particle sizes. Representative images are shown in Fig. 1, and particle sizing results are shown in Table 1. Sunscreens A and B
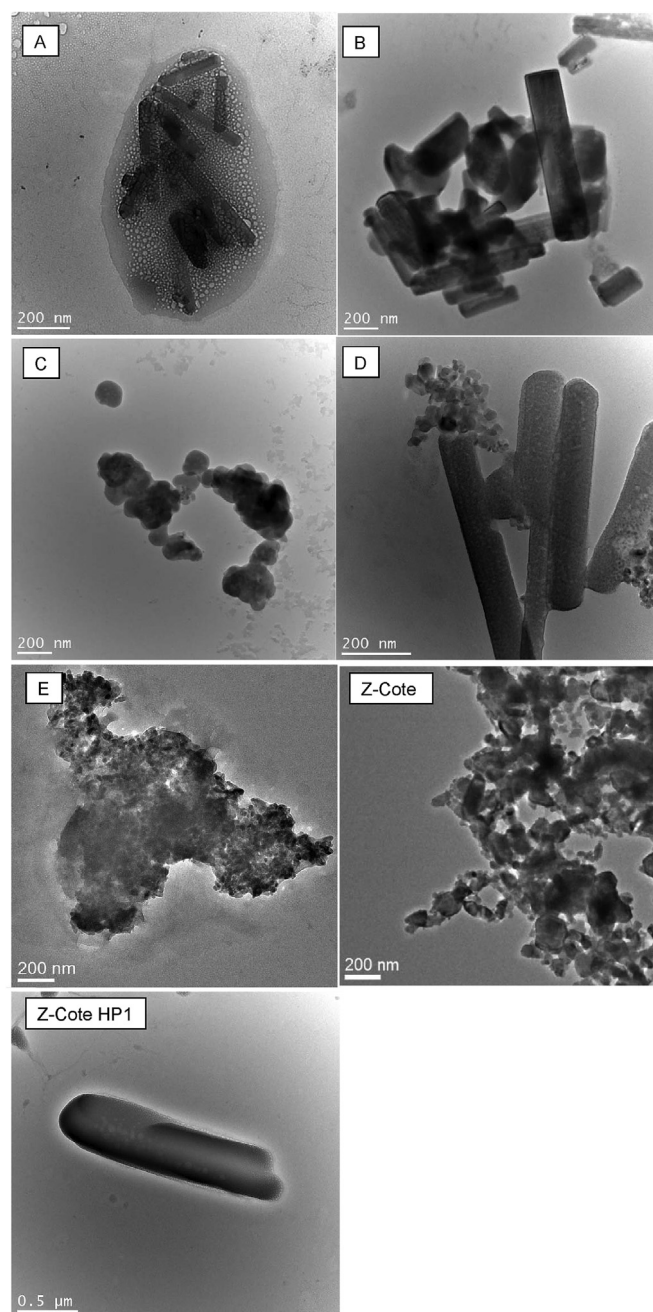
Fig. 1. TEM images of extracted sunscreens A, B, C, D, E and two as-purchased Z-Cote particles.

were mostly rod-shaped particles, while sunscreen E contained irregular or spherical particles. Sunscreen C contained mostly amorphous particles, and Sunscreen D contained rod-shaped Zn particles and amorphous Ti particles. Both Z-Cote formulations contained amorphous Zn particles, but particles in the HP1 formulation were slightly more rod shaped than the uncoated formulation. By TEM, the as-purchased sunscreens contained a significant amount of organic carbon, and these shapes were nearly absent in the particles extracted with DCM (Figure SI-2), indicating the extraction method removed the sunscreen matrix, leaving the metal oxide NP. For sunscreens A, C, and E, we also compared the particles size distribution of the extracted particles to the particles retained in the oil emulsion phase (Figure SI-1). Particle length and width distributions between the extracted particles and those that were not extracted for sunscreen A were not statistically different. The diameter of the extracted particles in sunscreen E was also not significantly different from the oil emulsion phase, but the amorphous particles extracted from sunscreen C were slightly greater in size than those retained in the emulsion layer (one-way ANOVA with Tukey's HSD, $p = 0.05$, Table 1). This may indicate that we selected for slightly larger particles during centrifugation in this specific sunscreen or that the particles aggregated differently between samples during drying of the TEM grid. Nonetheless, the extracted particles from sunscreen C were still relatively small (mean diameter = 136 nm) and relevant to environmental exposure studies.

We analyzed the particles by spICP-MS after dispersion of the particles into Milli-Q water and found that the measured Ti particle size distributions appear as folded-normal distributions (Figure SI-3), which indicated that a significant fraction of the particles were smaller than the minimum size detection limit of spICP-MS (i.e., smaller than 80 nm) (Lee et al., 2014). This is not surprising because the mean particle sizes found by TEM was <60 nm. We did not attempt to measure Zn nanoparticles because the particles sizes in the extracts and the size detection limit for Zn by spICP-MS are similar. Furthermore, the Zn NPs were clearly rod-shaped (Fig. 1), and spICP-MS calculations determine equivalent NP size using an assumption of spherical particles.

EDX analysis in each of the extracted samples showed that nearly all sunscreens contained either Ti or Zn particles, and the material matched well with the metal oxide on the label of the sunscreen. In one spectrum with extended counting time of sunscreen E, Si and Al were observed, which has previously been attributed to an organic and inorganic coating (Auffan et al., 2010). Si and Al were not observed in other sunscreen samples, but most EDX spectra were recorded with reduced counting time. An example of one representative sunscreen and an EDX spot analysis is shown in Figure SI-4. Confirmation of the expected metal oxides was conducted using XRD, and the peaks also matched well with the labeled metal oxide (either nZnO or nTiO$_2$). The peak positions and relative intensities for nTiO$_2$ and nZnO were referenced from the ICDD database (ZnO: 01-070-8072; TiO$_2$ (anatase): 01-070-6826; TiO$_2$ (rutile): 01-072-4814). The nTiO$_2$ crystallinity in sunscreens D and E was anatase and rutile, respectively (Figure SI-5). Z-Cote and Z-Cote HP1 contained peaks consistent with ZnO.

When the extracted particles were dispersed in water for aqueous experiments, we found that some particles were readily dispersible (extracted particles from sunscreens C and E, and Z-Cote, P25, and P90). Other NPs (particles extracted from sunscreens A, B, and D, and Z-Cote HP1) exhibited hydrophobic characteristics: poor dispersion in water after vortexing and sonication and instantaneous association with the walls of the polypropylene tube and at the air/water interface. The meniscus of the aqueous phase was also inverted (convex), indicating either a reduction in the surface affinity (repulsion) to the polypropylene coated with the NPs, or, less likely, greater affinity between the aqueous phase and the remaining suspended NPs. Notably, the label of sunscreens B and C described them as containing "Z-Cote", and the Z-Cote HP1 formulation is sold as a hydrophobic, polydimethylsiloxane (PDMS) coated formulation of Z-Cote nZnO particles. Others have also reported finding PDMS and Al(OH)$_3$ coatings on nanoparticles used in sunscreen formulations (Auffan et al., 2010). XRF confirmed that the as-received powder Z-Cote HP1 particles contained approximately 0.2% Si (detection limit = 0.02%), similar to the 2% found by Auffan et al. on another sunscreen formulation. In this study, Si in the uncoated Z-Cote formulation was below the XRF detection limit. We believe that a hydrophobic coating, potentially PDMS, was responsible for the hydrophobic characteristics of the particles extracted from sunscreens A, B, D, and Z-Cote HP1.

We expect little or no PDMS dissolution during extraction from the sunscreen because of the short contact periods with DCM. Although DCM may have caused some PDMS swelling during extraction, swelling was likely reversed during solvent removal (Lee et al., 2003). We assume that the three commercial sunscreens that exhibited strong hydrophobicity were likely to have similar coatings.

Other researchers were able to alter the hydrophobic PDMS coating on commercial nanoparticles in minutes by suspending them in pH 5 buffer solutions. The change in hydrophobicity was attributed to degradation of the Si-O-Si backbone and/or desorption of the polymer from the NP surface (Auffan et al., 2010). Our goal was not to completely remove the coating, but to stabilize the NPs in an environmentally relevant matrix while minimizing artificial changes to the materials and coatings. We placed the pellets of hydrophobic material into 0.1M pH 6 phosphate buffer and sonicated. 0.1M was selected as the buffer concentration to maintain sufficient buffering capacity in further experiments where the solutions are dilute (e.g., zebrafish exposures). The NPs were significantly more stable in solution at this pH. Although some settling occurred over 24 h, the solutions were still opaque. While the nanoparticles were relatively stable in solution at pH 6, we did not observe the same hydrophobicity change as the previous researchers after we washed out the pH 6 buffer and dispersed the particles in Milli-Q water, even after 1 month of storage. Thus, we elected to conduct aqueous studies at pH 6 for these sunscreens. We also selected for the most environmentally relevant particles by decanting a particle suspension after 24 h of settling in pH 6 buffer.

Overall, our findings of particle shape and size distribution are similar to previous findings. Zn particles were typically rod shaped, and Ti particles were smaller, either rod shaped (with slightly sharper edges, previously described as needle shaped (Lewicka et al., 2011)) or small spheres. The image of sunscreen D in Fig. 1, contained both Zn and Ti and provides an excellent example of this dichotomy.

3.2. Characterization of organic UV filters

Organic UV filters are generally small compounds and those studied here have molecular weight between 228 and 766 Da. The low aqueous solubility of the organic UV filters that afford them their water resistant properties also results in high octanol water partition coefficients (log K_{ow} ranging from 3.6 to 12.4 (Chemicalize.org, 2016)), physical/chemical characteristics of the organic UV filters contained in Tables SI-1). LogD values were calculated for each organic sunscreen for pH 8, and values ranging from −0.7 to >12 indicating lipophilicity, partitioning to fats, and likely bioaccumulation. Bioconcentration factors (BCF) calculated using EPISuite (US EPA, 2016) for each compound ranged from 3 to 16,120 L/kg. Notably, iscotrizinol and ecamsule had the lowest potential for bioaccumulation (3 L/kg) but are not approved for use in

the US. Although these are only predicted BCFs, several studies corroborate this evidence with environmental measurements (Bachelot et al., 2012; Buser et al., 2006; Tsui et al., 2017). Bioaccumulation of some nanoparticles has been reported (Hou et al., 2013; López-Serrano et al., 2014), but BCF values appear to be lower for NPs than many of the organic UV filter chemicals. Therefore, although it was not the goal of our experiments to determine chronic exposure trade-offs because there is already a significant effort in the literature aimed at this goal, it is notable that replacement of organic UV filters with NPs may reduce the potential ecological effects associated with chronic exposure and bioaccumulation of organic UV filters.

3.3. Zebrafish developmental effects

Zebrafish were exposed to nanoparticles extracted from sunscreens and to organic UV filters and our goal was to compare the tradeoffs of substituting NPs for organic chemicals to a potential environmental exposure endpoint (i.e., zebrafish embryos). The organic UV filters did not impact animal development over 5 days, even when tested at aqueous saturation, suggesting that estrogenic effects reported by others may be limited to specific susceptible species or repeated exposure (Coronado et al., 2008).

Three of the particle extracts (sunscreens A, B, and D) and Z-Cote, all which contain nZnO, resulted in statistically significant effects to the embryo development at the relatively high concentrations tested (Fig. 2, raw data contained in Tables SI–2). Both the particles from sunscreen B and D caused statistically significant mortality. Because we only observed effects in animals exposed to

Zn particles, these deviations from normal development may be due to Zn dissolution from the particle (i.e., Zn ion induced toxicity, rather than nZnO particles) (Bohme et al., 2017; Reed et al., 2012). Other samples were not tested at such elevated concentrations because the resulting particle extracts were not concentrated enough to allow for such high doses (i.e., lack of stable suspension during 24 h quiescent period) but also because exposures greater than 1 mg/L are not likely to be environmentally relevant. Overall, the concentrations dosed are considerably higher than would be expected in the environment. Thus, these nanoparticles are expected to have little or no impacts on zebrafish.

### 3.4. Photocatalytic properties of inorganic and organic UV filters

nZnO and nTiO$_2$ can be photocatalysts, which causes concern that the inorganic UV filters used in sunscreens may produce ROS on skin or in the environment when exposed to sunlight. To investigate this, we exposed the nanoparticles extracted from sunscreen to 302 nm light (25W) in the presence of a sacrificial MB dye. For P25, increasing NP dose and UV irradiation time led to greater MB oxidation. Pseudo-first order rate constants from each NP dose experiment were obtained (Figure SI-6) and used to determine pseudo second order rate constants (L mg^{-1} s^{-1}). As illustrated in Fig. 3 (full data set in Tables SI–3), P25 had slightly faster MB removal than P90, despite the smaller particle size of P90; neither P25 nor P90 are used in sunscreens but were analyzed to benchmark sunscreen NP reactivity.

Two of five sunscreens' NPs did not measurably oxidize MB. Three of the extracted particle suspensions oxidized MB with rate
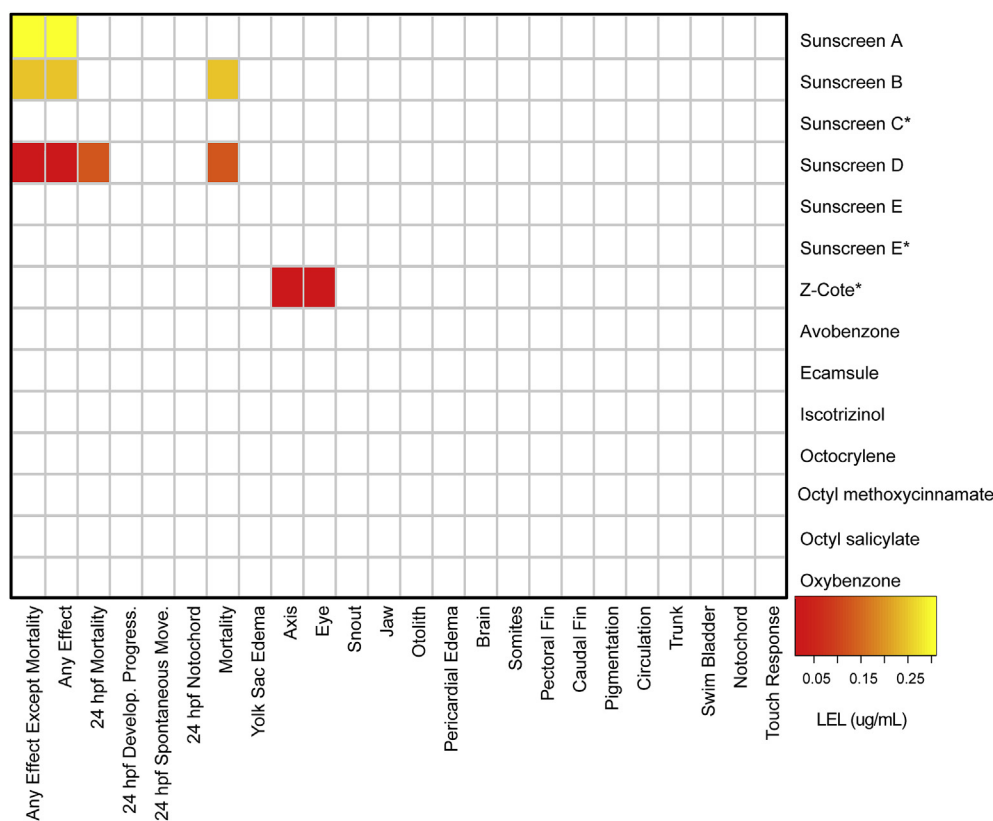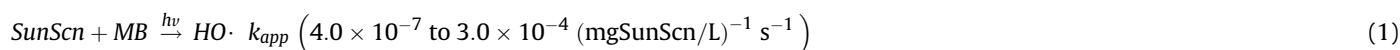

Fig. 2. Heatmap of sunscreen nanoparticles and organic UV filters lowest effect levels (LELs) on multiple zebrafish developmental endpoints. Zebrafish were exposed to organic UV filters at up to 5 μM, which is higher than the aqueous solubility limits, except for oxybenzone (predicted solubility 301 μM, Tables SI–1). The greatest exposure doses of the inorganic sunscreens were based on 1/100th of the extract concentration. Asterisks indicate stock solutions that were dispersed in Milli-Q water; all other samples were dispersed in pH 6 phosphate buffer. Lowest effect levels were calculated using an approach previously described by Truong et al. (2014) and the raw observation data is provided in Tables SI–2.
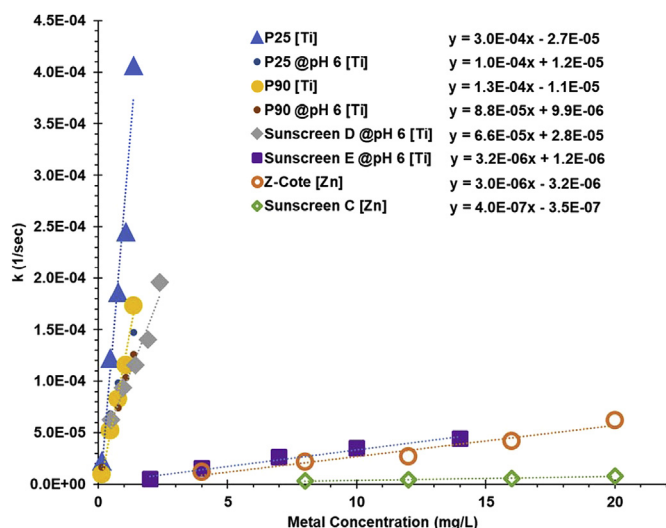
Fig. 3. First order rate constants for MB absorbance reduction as a function of NP concentration to yield slopes corresponding to 2nd order rate constants for $NP + MB \xrightarrow{h\nu}$ products during exposure. Note that sunscreen D contained both ZnO and TiO$_2$. Organic and inorganic UV filters with no measurable photoactivity are not shown.

constants from 4.0×10^{-7} to 6.6×10^{-5} L mg^{-1}·s^{-1}. Notably, the highest rate constants were obtained for sunscreens that contained TiO$_2$. The highest rate constant was obtained from sunscreen D, which contained both nZnO and nTiO$_2$ (Fig. 3, rate constant function of measured Ti). The nTiO$_2$ was anatase in crystallinity, which is more photoactive than rutile (Luttrell et al., 2014). Commercial photocatalysts P25 and P90 had rate constants greater than the sunscreen particles, from 1.3×10^{-4} to 3.0×10^{-4} L mg^{-1}·s^{-1}, and the presence of the pH buffer did not appear to extensively change the rate constant. The pH 6 buffered condition was selected to ensure UV exposure experiments conducted with buffered nanoparticle extracts were comparable to unbuffered samples, and to use the same conditions as the bioassays. For sunscreen E, MB was

capable of oxidizing MB in the presence of UV light despite the presence of a coating, or the coating is altered or removed during extraction and storage in a way that does not affect their hydrophobicity but allows for excited electrons to pass freely.

The light source used in our experiments produced 4.3–8 mW/cm^2 of UV irradiance at the illuminator surface, which is approximately 2–3 times the solar UV irradiance at ground level (2.6 mW/cm^2) (American Society for Testing and Materials, 2016; Gilmore et al., 1994; Hasinoff et al., 2001; Tan et al., 2014). NPs or organic sunscreens in the environment will be exposed to solar irradiance attenuated by the atmosphere (included in the above value) plus dissolved organic compounds and particles suspended in the water column. Our experiments show the likely trends in reactivity based upon NP source material, but the MB oxidation in our experiments is likely to be greater than would be expected in the environment.

None of the organic UV filters reacted with MB in the presence of UV light (<5% deviation from control), even up to aqueous saturation. Thus, incorporating nTiO$_2$ may be cause for concern if excited electrons are not properly captured by a coating or if the coating is susceptible to degradation.

3.5. Environmental implications of sunscreen use

Two environmental impacts could occur in aquatic systems. First, our experiments and others have shown limited toxicity to zebrafish, algae, daphnia, and other organisms in the presence of nTiO$_2$ and nZnO (Aruoja et al., 2009; Baun et al., 2008; Rampaul et al., 2007; Reed et al., 2012). Second, the photocatalytic potential of NPs used in sunscreens is highly variable, which may cause environmental exposure to ROS, and this is ignored in normal toxicity testing.

Using the apparent rate constants (Fig. 3) for MB loss during irradiation of nanoscale metal oxides contained in sunscreens (SunScn), we can estimate the steady state hydroxyl radical (HO·) concentration, following similar approaches developed by Page et al. and Dong et al. for photosensitized oxidation of pollutants by natural organic matter (NOM) (Dong et al., 2015; Page et al., 2011). The observed experimental reaction includes both HO· production and MB reactions:

$$SunScn + MB \xrightarrow{h\nu} HO \cdot \quad k_{app} \left(4.0 \times 10^{-7} \text{ to } 3.0 \times 10^{-4} \text{ (mgSunScn/L)}^{-1} \text{ s}^{-1} \right) \tag{1}$$

degraded in the pH 6 buffer but not in Milli-Q water (<5% deviation from control). The acidic buffer may have removed a coating on the particle that inhibited photocatalytic activity. Although the particles extracted from commercial sunscreens were less reactive than commercial photocatalysts, the most reactive particles were, predictably, anatase phase TiO$_2$.

The uncoated material Z-Cote had low photoactivity, and the PDMS coated Z-Cote HP1 was not photoactive in this assay, which suggests that the coating ceases oxidative species production during UV light exposure. Particles extracted from sunscreens that contained only zinc were either not measurably photoactive or had low photoactivity. The particles extracted from sunscreen D were exceptionally hydrophobic, requiring an acidic buffer for dispersion, which has been shown to partially desorb or shorten the Si-O-Si backbone of the PDMS coating (Auffan et al., 2010). Because of the hydrophobicity, we believe the particles retained their coating, and yet, the particles oxidized MB when exposed to UV light. Therefore, the nTiO$_2$ contained in sunscreen D produced ROS
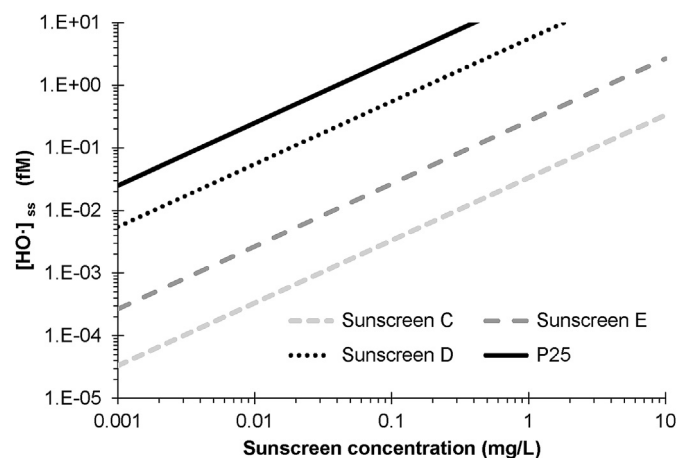
which yields:

$$\frac{d[MB]}{dt} = -k_{app}[SunScn][MB] \tag{2}$$

The second order rate constant for HO· with MB is known from pulse radiolysis experiments (Kishore et al., 1989):

$$MB + HO \cdot \rightarrow products \quad k_{HO\cdot, MB} = 1.2 \times 10^{10} \text{ M}^{-1} \text{ s}^{-1} \tag{3}$$
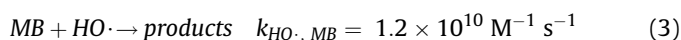
Which yields:

$$\frac{d[MB]}{dt} = -k_{HO\cdot, MB}[HO\cdot][MB] \tag{4}$$

Equations (2) and (4) must be equivalent and can be solved to yield the HO· concentration at any time:

Fig. 4. Steady state concentrations of hydroxyl radicals modeled using equation (5). Calculations are conducted using k_{app} from our UV light source, which is approximately 2–3 times more powerful than solar UV irradiance.

$$[HO\cdot]_{ss} = \frac{k_{app}[SunScn]}{k_{HO\cdot,\,MB}} \qquad (5)$$

Fig. 4 shows predictions of steady state HO· production from our experiments. At 1 mg/L nanoparticle concentration, between 0.01 and 10 fM of $[HO\cdot]_{ss}$ could form. The highest $[HO\cdot]_{ss}$ would occur from P90 with sunscreen extracted nanoparticles exhibiting orders of magnitude lower $[HO\cdot]_{ss}$ levels. For comparison, Page et al. (2010) reported $[HO\cdot]_{ss}$ on the order of 0.5–5 fM during 365 nm irradiation of fulvic acids in the presence of 10 μM of a probe molecule because of their ability to form and quench HO· radicals. Thus, at least in comparing these two experiments, sunscreen metals would need to be present between 1 and 10 mg/L to be as reactive as radical species formed from photo-excited fulvic acids. These concentrations are higher than the 10–100 μg/L TiO₂ present in wastewater effluents and what has been reported in waters used heavily for recreation (Gondikas et al., 2014; Kiser et al., 2009). In contrast, P25 concentrations of 0.02–0.2 mg/L could produce as much HO· as the fulvic acids, although these concentrations are not likely in wastewater effluents. Furthermore, it is unlikely that sunlight capable of exciting nTiO₂ or nZnO (<380 nm) would penetrate deeply into natural waters because the photons are absorbed by dissolved organic matter and the UV output of the lamp used to model k_{app} is 2–3 times more energetic than solar irradiance. However, in spill or other unique scenarios with high releases of sunscreens and their respective metal oxides, or low dissolved organic matter concentrations, the presence or accumulation of sunscreens could result in low level production of HO·. Because the materials are catalysts, they would likely continue to produce these radicals over long periods of time. Finally, nano-scale metal oxides are used in conjunction with organic UV filters, rather than the sole UV filter, and so any environmental effects of nano-scale metal oxide releases from sunscreens are additive to the effects of organic UV filters.

4. Conclusions

Nano-scale TiO₂ and ZnO have been incorporated into sunscreens over the past two decades because they have favorable UV-filtering and tactile profiles, and are invisible to the human eye. However, nTiO₂ and nZnO can be semiconductor photocatalysts. We examined the ecological implications of NP release from sunscreens and found the following:

- Metal oxides in sunscreens matched well with the labeled metal oxide active ingredient, either nZnO or nTiO₂, and were extractable from the organic matrix using solvent washing and centrifugation.
- Some NPs contained in sunscreens were hydrophobic, likely a result of a polymer coating containing silica. Reduced pH stabilized the NPs.
- The organic UV filters studied here were not developmentally toxic to zebrafish, even up to aqueous saturation. Zinc particles were more toxic to zebrafish embryogenesis than titanium, although the concentrations at which this occurred were higher than would be expected in the environment.
- Organic UV filters have the potential to bioaccumulate, which is the subject of multiple other studies, and was not the focus of this research.
- nTiO₂ and nZnO extracted from sunscreens measurably degrade MB when exposed to UV light, but we estimate the ROS produced under normal release scenarios from wastewater or recreational bathing is lower than that produced by naturally occurring organic matter.

Overall, we find that the incorporation of NP into sunscreens has limited ecological risk to the endpoints we selected. However, considering that NP are typically used in sunscreens alongside organic UV filters, the risks associated with NP, albeit small, are additive to that of organic UV filters. Should NP completely replace organic UV filters, concerns of zinc dissolution and environmental ROS production may begin to replace concerns of bioaccumulation and estrogenic activity of organic UV filters following the rise in NP concentrations and fall of organic UV filter concentrations in the environment.

Appendix A. Supplementary data

Supplementary data related to this article can be found at https://doi.org/10.1016/j.watres.2018.03.062.

References

American Society for Testing and Materials, 2016. G173–03 Reference Spectra Derived from Smarts V. 2.9.2.

Aruoja, V., Dubourguier, H.-C., Kasemets, K., Kahru, A., 2009. Toxicity of nanoparticles of Cuo, Zno and Tio2 to microalgae pseudokirchneriella subcapitata. Sci. Total Environ. 407 (4), 1461–1468.

Auffan, M., Pedeutour, M., Rose, J., Masion, A., Ziarelli, F., Borschneck, D., Chaneac, C., Botta, C., Chaurand, P., Labille, J., Bottero, J.-Y., 2010. Structural degradation at the surface of a Tio2-based nanomaterial used in cosmetics. Environ. Sci. Technol. 44 (7), 2689–2694.

Bachelot, M., Li, Z., Munaron, D., Le Gall, P., Casellas, C., Fenet, H., Gomez, E., 2012. Organic uv filter concentrations in marine mussels from French coastal regions. Sci. Total Environ. 420, 273–279.

Balmer, M.E., Buser, H.R., Muller, M.D., Poiger, T., 2005. Occurrence of some organic uv filters in wastewater, in surface waters, and in fish from swiss lakes. Environ. Sci. Technol. 39 (4), 953–962.

Barker, P.J., Branch, A., 2008. The interaction of modern sunscreen formulations with surface coatings. Prog. Org. Coating 62 (3), 313–320.

Baun, A., Hartmann, N.B., Grieger, K., Kusk, K.O., 2008. Ecotoxicity of engineered

nanoparticles to aquatic invertebrates: a brief review and recommendations for future toxicity testing. Ecotoxicology 17 (5), 387–395.

Bohme, S., Baccaro, M., Schmidt, M., Potthoff, A., Stark, H.-J., Reemtsma, T., Kuhnel, D., 2017. Metal uptake and distribution in the zebrafish (Danio Rerio) embryo: differences between nanoparticles and metal ions. Environ. Sci.: Nano 4 (5), 1005–1015.

Bouchard, D., Knightes, C., Chang, X., Avant, B., 2017. Simulating multiwalled carbon nanotube transport in surface water systems using the water quality analysis simulation program (wasp). Environ. Sci. Technol. 51 (19), 11174–11184.

Buser, H.-R., Balmer, M.E., Schmid, P., Kohler, M., 2006. Occurrence of uv filters 4-methylbenzylidene camphor and octocrylene in fish from various swiss rivers with inputs from wastewater treatment plants. Environ. Sci. Technol. 40 (5), 1427–1431.

Chemicalizeorg, 2016. Marvin Was Used for Drawing, Displaying, and Prediction of Chemicals and Properties. Marvin v15.12.14. http://chemaxon.com.

Cokkinides, V., Weinstock, M., Glanz, K., Albano, J., Ward, E., Thun, M., 2006. Trends in sunburns, sun protection practices, and attitudes toward sun exposure protection and tanning among us adolescents, 1998–2004. Pediatrics 118 (3), 853.

Coronado, M., De Haro, H., Deng, X., Rempel, M.A., Lavado, R., Schlenk, D., 2008. Estrogenic activity and reproductive effects of the uv-filter oxybenzone (2-hydroxy-4-methoxyphenyl-methanone) in fish. Aquat. Toxicol. 90 (3), 182–187.

David Holbrook, R., Motabar, D., Quiñones, O., Stanford, B., Vanderford, B., Moss, D., 2013. Titanium distribution in swimming pool water is dominated by dissolved species. Environ. Pollut. 181, 68–74.

Dong, M.M., Trenholm, R., Rosario-Ortiz, F.L., 2015. Photochemical degradation of atenolol, carbamazepine, meprobamate, phenytoin and primidone in wastewater effluents. J. Hazard. Mater. 282, 216–223.

Dunford, R., Salinaro, A., Cai, L., Serpone, N., Horikoshi, S., Hidaka, H., Knowland, J., 1997. Chemical oxidation and DNA damage catalysed by inorganic sunscreen ingredients. FEBS Lett. 418 (1–2), 87–90.

European Comission, 2009. Regulation (Ec) No 1223/2009 O the European Parliament and of the Council.

Foltète, A.-S., Masfaraud, J.-F., Bigorgne, E., Nahmani, J., Chaurand, P., Botta, C., Labille, J., Rose, J., Férard, J.-F., Cotelle, S., 2011. Environmental impact of sunscreen nanomaterials: ecotoxicity and genotoxicity of altered Tio2 nanocomposites on Vicia Faba. Environ. Pollut. 159 (10), 2515–2522.

Food and Drug Administration, 2016a. Sunscreen Drug Products for Over-the-Counter Human Use. 21CFR352.10.

Food and Drug Administration, 2016b. Fda Basics: what Does the Fda Do?.

Fouqueray, M., Dufils, B., Vollat, B., Chaurand, P., Botta, C., Abacci, K., Labille, J., Rose, J., Garric, J., 2012. Effects of aged Tio2 nanomaterial from sunscreen on Daphnia magna exposed by dietary route. Environ. Pollut. 163, 55–61.

Garner, K.L., Suh, S., Keller, A.A., 2017. Assessing the risk of engineered nanomaterials in the environment: development and application of the nanofate model. Environ. Sci. Technol. 51 (10), 5541–5551.

Gilmore, W., Correale, J., Weiner, L.P., 1994. Coronavirus induction of class I major histocompatibility complex expression in murine astrocytes is virus strain specific. J. Exp. Med. 180 (3), 1013.

Gondikas, A.P., Kammer, F.v.d., Reed, R.B., Wagner, S., Ranville, J.F., Hofmann, T., 2014. Release of Tio2 nanoparticles from sunscreens into surface waters: a one-year survey at the old danube recreational lake. Environ. Sci. Technol. 48 (10), 5415–5422.

Gottschalk, F., Sun, T., Nowack, B., 2013. Environmental concentrations of engineered nanomaterials: review of modeling and analytical studies. Environ. Pollut. 181, 287–300.

Gulson, B., McCall, M., Korsch, M., Gomez, L., Casey, P., Oytam, Y., Taylor, A., McCulloch, M., Trotter, J., Kinsley, L., Greenoak, G., 2010. Small amounts of zinc from zinc oxide particles in sunscreens applied outdoors are absorbed through human skin. Toxicol. Sci. 118 (1), 140–149.

Hasinoff, B.B., Chee, G.-L., Day, B.W., Avor, K.S., Barnabé, N., Thampatty, P., Yalowich, J.C., 2001. Synthesis and biological activity of a photoaffinity etoposide probe. Bioorg. Med. Chem. 9 (7), 1765–1771.

Hayden, C.G., Roberts, M.S., Benson, H.A., 1997. Systemic absorption of sunscreen after topical application. Lancet 350 (9081), 863–864.

Hayden, C.G.J., Cross, S.E., Anderson, C., Saunders, N.A., Roberts, M.S., 2005. Sunscreen penetration of human skin and related keratinocyte toxicity after topical application. Skin Pharmacol. Physiol. 18 (4), 170–174.

Hjorth, R., Hansen, S.F., Jacobs, M., Tickner, J., Ellenbecker, M., Baun, A., 2016. The applicability of chemical alternatives assessment for engineered nanomaterials. Integrated Environ. Assess. Manag. 13 (1), 177–187.

Hou, W.-C., Westerhoff, P., Posner, J.D., 2013. Biological accumulation of engineered nanomaterials: a review of current knowledge. Environ. Sci.: Process. Impacts 15 (1), 103–122.

Johnson, A.C., Bowes, M.J., Crossley, A., Jarvie, H.P., Jurkschat, K., Jürgens, M.D., Lawlor, A.J., Park, B., Rowland, P., Spurgeon, D., Svendsen, C., Thompson, I.P., Barnes, R.J., Williams, R.J., Xu, N., 2011. An assessment of the fate, behaviour and environmental risk associated with sunscreen Tio2 nanoparticles in UK field scenarios. Sci. Total Environ. 409 (13), 2503–2510.

Kiser, M., Westerhoff, P., Benn, T., Wang, Y., Perez-Rivera, J., Hristovski, K., 2009. Titanium nanomaterial removal and release from wastewater treatment plants. Environ. Sci. Technol. 43 (17), 6757–6763.

Kishore, K., Guha, S.N., Mahadevan, J., Moorthy, P.N., Mittal, J.P., 1989. Redox reactions of methylene blue: a pulse radiolysis study. Int. J. Radiat. Appl. Instrum. Part C. Radiat. Phys. Chem. 34 (4), 721–727.

Kupper, T., Plagellat, C., Brändli, R.C., de Alencastro, L.F., Grandjean, D., Tarradellas, J.,

2006. Fate and removal of polycyclic musks, uv filters and biocides during wastewater treatment. Water Res. 40 (14), 2603–2612.

Labille, J., Feng, J., Botta, C., Borschneck, D., Sammut, M., Cabie, M., Auffan, M., Rose, J., Bottero, J.-Y., 2010. Aging of Tio2 nanocomposites used in sunscreen. Dispersion and fate of the degradation products in aqueous environment. Environ. Pollut. 158 (12), 3482–3489.

Lee, J.N., Park, C., Whitesides, G.M., 2003. Solvent compatibility of poly(dimethylsiloxane)-based microfluidic devices. Anal. Chem. 75 (23), 6544–6554.

Lee, N.A., Kim, S.J., Park, B.J., Park, H.M., Yoon, M., Chung, B.H., Song, N.W., 2011. Development of multiplexed analysis for the photocatalytic activities of nanoparticles in aqueous suspension. Photochem. Photobiol. Sci. 10 (12), 1979–1982.

Lee, S., Bi, X., Reed, R.B., Ranville, J.F., Herckes, P., Westerhoff, P., 2014. Nanoparticle size detection limits by single particle icp-ms for 40 elements. Environ. Sci. Technol. 48 (17), 10291–10300.

Lewicka, Z.A., Benedetto, A.F., Benoit, D.N., Yu, W.W., Fortner, J.D., Colvin, V.L., 2011. The structure, composition, and dimensions of Tio2 and Zno nanomaterials in commercial sunscreens. J. Nanoparticle Res. 13 (9), 3607–3617.

Liu, H.H., Cohen, Y., 2014. Multimedia environmental distribution of engineered nanomaterials. Environ. Sci. Technol. 48 (6), 3281–3292.

López-Serrano, A., Muñoz-Olivas, R., Sanz-Landaluze, J., Olasagasti, M., Rainieri, S., Cámara, C., 2014. Comparison of bioconcentration of ionic silver and silver nanoparticles in zebrafish eleutheroembryos. Environ. Pollut. 191, 207–214.

Luttrell, T., Halpegamage, S., Tao, J., Kramer, A., Sutter, E., Batzill, M., 2014. Why is anatase a better photocatalyst than Rutile? - model studies on epitaxial Tio2 films. Sci. Rep. 4, 4043.

Meesters, J.A., Koelmans, A.A., Quik, J.T., Hendriks, A.J., van de Meent, D., 2014. Multimedia modeling of engineered nanoparticles with Simplebox4nano: model definition and evaluation. Environ. Sci. Technol. 48 (10), 5726–5736.

Mueller, N.C., Nowack, B., 2008. Exposure modeling of engineered nanoparticles in the environment. Environ. Sci. Technol. 42 (12), 4447–4453.

Pace, H.E., Rogers, N.J., Jarolimek, C., Coleman, V.A., Higgins, C.P., Ranville, J.F., 2011. Determining transport efficiency for the purpose of counting and sizing nanoparticles via single particle inductively coupled plasma mass spectrometry. Anal. Chem. 83 (24), 9361–9369.

Page, S.E., Arnold, W.A., McNeill, K., 2010. Terephthalate as a probe for photochemically generated hydroxyl radical. J. Environ. Monit. 12 (9), 1658–1665.

Page, S.E., Arnold, W.A., McNeill, K., 2011. Assessing the contribution of free hydroxyl radical in organic matter-sensitized photohydroxylation reactions. Environ. Sci. Technol. 45 (7), 2818–2825.

Poiger, T., Buser, H.-R., Balmer, M.E., Bergqvist, P.-A., Müller, M.D., 2004. Occurrence of uv filter compounds from sunscreens in surface waters: regional mass balance in two swiss lakes. Chemosphere 55 (7), 951–963.

Praetorius, A., Scheringer, M., Hungerbühler, K., 2012. Development of environmental fate models for engineered nanoparticles —a case study of Tio2 nanoparticles in the rhine river. Environ. Sci. Technol. 46 (12), 6705–6713.

Rampaul, A., Parkin, I.P., Cramer, L.P., 2007. Damaging and protective properties of inorganic components of sunscreens applied to cultured human skin cells. J. Photochem. Photobiol. Chem. 191 (2–3), 138–148.

Reed, R.B., Ladner, D.A., Higgins, C.P., Westerhoff, P., Ranville, J.F., 2012. Solubility of nano-zinc oxide in environmentally and biologically important matrices. Environ. Toxicol. Chem. 31 (1), 93–99.

Reif, D.M., Truong, L., Mandrell, D., Marvel, S., Zhang, G., Tanguay, R.L., 2016. High-throughput characterization of chemical-associated embryonic behavioral changes predicts teratogenic outcomes. Arch. Toxicol. 90 (6), 1459–1470.

Robinson, J.K., Rigel, D.S., Amonette, R.A., 1997. Trends in sun exposure knowledge, attitudes, and behaviors: 1986 to 1996. J. Am. Acad. Dermatol. 37 (2, Part 1), 179–186.

Sadrieh, N., Wokovich, A.M., Gopee, N.V., Zheng, J., Haines, D., Parmiter, D., Siitonen, P.H., Cozart, C.R., Patri, A.K., McNeil, S.E., Howard, P.C., Doub, W.H., Buhse, L.F., 2010. Lack of significant dermal penetration of titanium dioxide from sunscreen formulations containing nano- and submicron-size Tio2 particles. Toxicol. Sci. 115 (1), 156–166.

Schlumpf, M., Cotton, B., Conscience, M., Haller, V., Steinmann, B., Lichtensteiger, W., 2001. Vitro and in vivo estrogenicity of uv screens. Environ. Health Perspect. 109 (3), 239.

Schlumpf, M., Durrer, S., Faass, O., Ehnes, C., Fuetsch, M., Gaille, C., Henseler, M., Hofkamp, L., Maerkel, K., Reolon, S., Timms, B., Tresguerres, J.A.F., Lichtensteiger, W., 2008. Developmental toxicity of uv filters and environmental exposure: a review. Int. J. Androl. 31 (2), 144–151.

Tan, T.T.Y., Ahsan, A., Reithofer, M.R., Tay, S.W., Tan, S.Y., Hor, T.S.A., Chin, J.M., Chew, B.K.J., Wang, X., 2014. Photoresponsive liquid marbles and dry water. Langmuir 30 (12), 3448–3454.

Treffel, P., Gabard, B., 1996. Skin penetration and sun protection factor of ultra-violet filters from two vehicles. Pharmaceut. Res. 13 (5), 770–774.

Truong, L., Harper, S.L., Tanguay, R.L., 2011. In: Gautier, J.-C. (Ed.), Drug Safety Evaluation: Methods and Protocols. Humana Press, Totowa, NJ, pp. 271–279.

Truong, L., Reif, D.M., St Mary, L., Geier, M.C., Truong, H.D., Tanguay, R.L., 2014. Multidimensional in vivo hazard assessment using zebrafish. Toxicol. Sci. 137 (1), 212–233.

Tsui, M.M., Lam, J.C., Ng, T.Y., Ang, P.O., Murphy, M.B., Lam, P.K.-S., 2017. Occurrence, distribution and fate of organic uv filters in coral communities. Environ. Sci. Technol. 51 (8), 4182–4190.

Urbach, F., 2001. The historical aspects of sunscreens. J. Photochem. Photobiol. B Biol. 64 (2–3), 99–104.

US EPA, 2016. Esitmation Programs Interface Suite™ for Microsoft® Windows, V 4.11. United States Environmental Protection Agency, Washington, Dc, USA.

Venkatesan, A.K., Reed, R.B., Lee, S., Bi, X., Hanigan, D., Yang, Y., Ranville, J.F., Herckes, P., Westerhoff, P., 2018. Detection and sizing of Ti-Containing particles in recreational waters using single particle icp-ms. Bull. Environ. Contam. Toxicol. 100 (1) , 120–126.

Westerhoff, P., Nowack, B., 2013. Searching for global descriptors of engineered nanomaterial fate and transport in the environment. Acc. Chem. Res. 46 (3), 844–853.